Volume 58
Number 25
28 March 2022
Pages 3983–4104

ChemComm

Chemical Communications

rsc.li/chemcomm

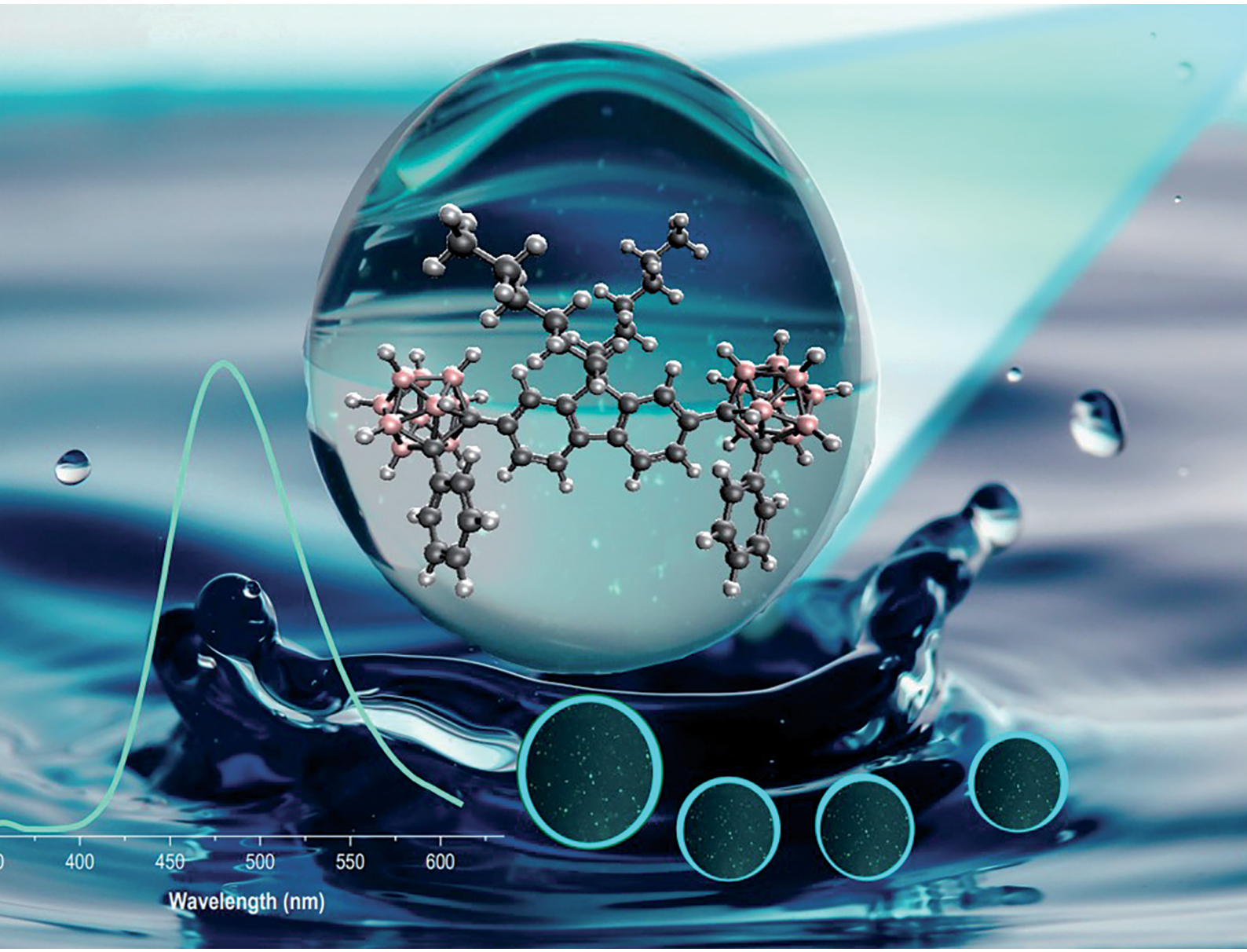

ISSN 1359-7345

ROYAL SOCIETY OF CHEMISTRY

COMMUNICATION

Rosario Núñez *et al.*

o-Carborane-based fluorophores as efficient luminescent systems both as solids and as water-dispersible nanoparticles

ChemComm

COMMUNICATION

View Article Online
View Journal | View Issue

Cite this: *Chem. Commun.*, 2022, **58**, 4016

Received 23rd December 2021,
Accepted 24th February 2022

DOI: 10.1039/d1cc07211k

rsc.li/chemcomm

o-Carborane-based fluorophores as efficient luminescent systems both as solids and as water-dispersible nanoparticles†‡

Sohini Sinha, [a] Zsolt Kelemen, [b] Evelyn Hümpfner, [b] Imma Ratera, [ac] Jean-Pierre Malval, [d] José Piers Jurado, [a] Clara Viñas, [a] Francesc Teixidor [a] and Rosario Núñez *[a]

A set of *o*-carborane-appended π-conjugated fluorophores and their light-emitting properties in the solid state are reported. The aggregation-induced emission enhancement (AIEE) exhibited for one of the fluorenyl derivatives paved the way to successfully preparing *o*-carborane-containing organic nanoparticles (NPs) homogeneously dispersed in aqueous media that maintain their luminescence properties. Notably, NPs processed as thin films also show high fluorescence efficiency, suggesting potential optical and optoelectronic applications.

Nowadays, the development of active light-emitting molecular materials for optoelectronic devices, such as organic light-emitting diodes, solar cells or semiconductors, is a major challenge.[1] The π-conjugated organic molecules are excellent building blocks for constructing solid-state luminescent materials. However, a common problem is aggregation-caused quenching (ACQ), commonly due to intermolecular π–π stacking interactions between the organic fragments, causing a serious impediment towards practical applications.[2] Such π–π stacking and the corresponding ACQ can be avoided by introducing 3D *ortho*-carborane clusters ($C_2B_{10}H_{12}$) to π-conjugated derivatives. The introduction of *o*-carborane not only prevents ACQ but also facilitates the phenomenon of aggregation-induced emission (AIE) to build efficient solid-state luminescent materials, enabling their use as optoelectronic devices.[3,4] The ability of the *o*-carborane cluster to cause AIE has been attributed to its 3D aromaticity, high chemical and thermal stability, and electronic properties.[5,6] The strong electron-acceptor capacity of the cluster and its highly polarizable σ-aromatic character induce intramolecular charge transfer (ICT) between the π-conjugated aromatic groups and *o*-carborane.[7,8] Structural changes and geometries in the molecule can also affect the ICT transitions. A major drawback of these systems is, however, the lack of luminescence in solution due to quenching by non-radiative pathways.[9] The latter prevents them from being used in other appealing applications. This is particularly relevant in the case of bio(nano)medicine applications, where emissive properties in aqueous media are essential. So, we are currently interested in developing water soluble carborane-containing derivatives as theranostic agents for bioimaging and cancer treatment by boron neutron capture therapy (BNCT).[10] This further gets complicated by the insolubility of carboranes in water, as a consequence of their high hydrophobicity. So, a major challenge in this field is to provide carborane-based aggregation-induced emission luminogens (AIEgens) that can show efficient luminescence, both in the solid state and in aqueous solutions.

To overcome the above-mentioned drawbacks, herein we have proposed that carborane-based AIEgens in the solid state can be transformed to water-dispersible nanoparticles, while maintaining the AIE luminescence properties. Thus, we have selected fluorene and thiophene as donor (D) groups to couple onto electron-acceptor *o*-carborane clusters, due to their aromaticity and ease of functionalisation.[11] We have explored the photophysical behavior of the new compounds in different states such as solution, solid, aggregation and water suspension. In particular, we have successfully prepared luminescent and stable *o*-carborane-based organic NPs homogenously dispersed in aqueous media, for the first time. This also allowed us to prepare films that exhibit high fluorescence quantum

[a] *Institut de Ciència de Materials de Barcelona (ICMAB-CSIC), Campus U.A.B., 08193, Bellaterra, Barcelona, Spain. E-mail: rosario@icmab.es*
[b] *Department of Inorganic and Analytical Chemistry, Budapest University of Technology and Economics, Műegyetem Rkp 3, H-1111 Budapest, Hungary*
[c] *CIBER de Bioingeniería, Biomateriales y Nanomedicina (CIBER-BBN), 28029 Madrid, Spain*
[d] *Université de Haute-Alsace, Institut de Science des Matériaux de Mulhouse (CNRS-UMR7361), 15 rue Jean Starcky BP 2488, 68057 Mulhouse, France*

† S. S, Z. K., I. R. and R. N. dedicate this work to Professors Francesc Teixidor and Clara Viñas on the occasion of their 70th birthdays and in recognition of their valuable contributions to boron chemistry over the last 40 years, including hosting EUROBORON and IMEBORON conferences.

‡ Electronic supplementary information (ESI) available: Experimental details, NMR spectra, DFT calculations, and photophysical data. See DOI: 10.1039/d1cc07211k

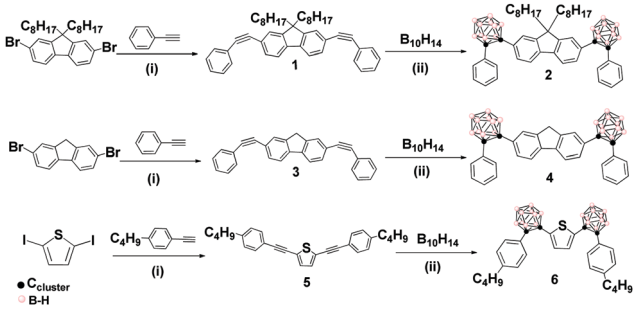

Scheme 1 Synthesis of fluorene- and thiophene-based π-conjugated systems linked to *o*-carborane clusters: (i) $Pd(PPh_3)_2Cl_2$, CuI, TEA and toluene (1 : 9 v/v); (ii) 5 eq. Et_2S, toluene, 72 h, and 110 °C.

yields. Precursors **1**, **3** and **5** have been synthesized by Pd-catalyzed Sonogashira cross-coupling reaction (Scheme 1).[12] Then, the insertion reaction of **1** and **3** with decaborane ($B_{10}H_{14}$) was performed using optimized conditions (see the ESI‡ for details) to obtain **2** and **4** with moderate yields (34% and 38%, respectively, Scheme 1). The carboranyl-containing thiophene **6** was synthesised with 32% yield by the insertion reaction of **5** with $B_{10}H_{14}$, following the same procedure (ESI‡). The structures of **1–6** were established on the basis of FT-IR, ^1H, $^{13}C\{^1H\}$ and $^{11}B\{^1H\}$ spectroscopic techniques and elemental analysis (ESI‡ and Fig. S1–S15).

Fluorene precursors **1** and **3** exhibit intense absorption bands with maxima at 349 and 346 nm, respectively, which undergo dramatic blue-shifts (31–35 nm) for the carboranyl derivatives **2** and **4** (Fig. 1a and Table 1). The absorption bands mainly involve π–π* transitions of the fluorene rings. The blue-shifts, observed for **2** and **4** along with decreases in ε values, indicate a decrease in the conjugation for these systems.[11] The absorption spectra of **2** and **4** featuring low-energy absorption bands at 314 and 308 nm tailed off around 350 nm (Fig. 1a). These bands could be assigned to the transitions originating from the ICT between fluorene and the *o*-carborane moieties. To verify these hypotheses a computational study using different DFT functions was carried out (Tables S1 and S2, ESI‡). Investigating the canonical Kohn–Sham molecular orbitals, it can be established that the carborane units significantly break the conjugation between the π-conjugated units (Tables S3–S13, ESI‡). TD-DFT calculations have demonstrated that the observed absorption maxima (Fig. S16, ESI‡) are mainly due to the HOMO–LUMO transitions. The transitions of a pure organic system imply a long range π–π* type electronic delocalisation; however in the *o*-carborane-based compounds different ICT characteristics can be observed. Compound **5** shows an absorption maximum at 348 nm, which sustained a significant blue-shift after the incorporation of the *o*-carborane moiety in **6** (274 nm). The origin of this shift was verified by TD-DFT calculations and was attributed to the more significant charge transfer character of the corresponding transition. In **2** and **4**, the nature of the excitation has moderate ICT character, which goes from the fluorene units towards the carborane clusters, whereas in **6** the transition has very significant ICT character moving from the two phenyl rings towards the thiophene unit. In addition, the quadrupole nature of the structures of these systems prompted us to study their two-photon absorption properties (2PA) (details in the ESI‡).

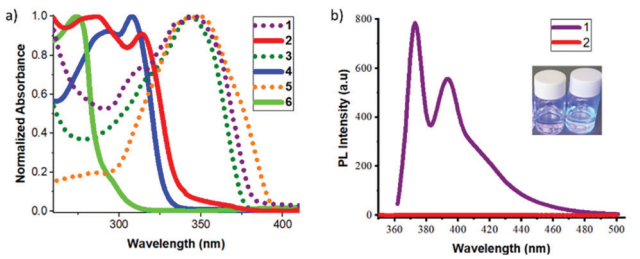

Fig. 1 (a) UV-Vis spectra of **1–6** in THF (3×10^{-5} M to $1{\cdot}10^{-6}$ M). (b) Fluorescence emission spectra of **1** and **2** in THF (3×10^{-5} M to 1×10^{-6} M). Inset: Solutions of **1** and **2** in THF ander UV irradiation.

Precursors **1** and **3** exhibit two emission maxima at 372 and 367 nm with fluorescence quantum yields (Φ_{PL}) of 0.89 and 0.64, respectively. After the incorporation of the *o*-carborane clusters, a significant fluorescence quenching was observed with negligible Φ_{PL} for **2** and **4** in THF solution (Table 1 and the ESI‡). A comparative plot of the fluorescence emission spectra of **1** and **2** in THF is shown in Fig. 1b. This result was in full agreement with the DFT calculations, confirming an ICT to the *o*-carborane unit that causes fluorescence quenching (Fig. S17, ESI‡). On the contrary, no significant changes in the emission patterns for the thiophene derivatives **5** and **6** were observed and this could be explained by the different nature of the excitation. In compound **6**, the ICT occurs from the two phenyl rings towards the thiophene unit and the participation of the carborane cluster in the ICT process is minor. Indeed, no quenching in solution nor AIE in the aggregate state could be expected (*vide infra*).

Photoluminescence (PL) behaviour of **2**, **4** and **6** in aggregates (THF/H_2O = 1 : 99 (v/v)), solid states and film (ESI‡) was also investigated (Fig. 2 and Table 1). Significant differences were found for the three compounds and only compound **2**, with the octyl chain, showed an enhanced fluorescence emission. The PL spectra of **2** showed a non-vibronic structure with a maximum at 477 nm in the solid state and 473 nm in the film state, which were around 70 nm red-shifted from the THF solution (Table 1). This result confirms that the luminescence mechanism is related to the ICT between *o*-carboranes and the fluorene unit.[11] Remarkably, the fluorescence efficiencies with Φ_{PL} values of 0.71 and 0.74 in solid and film, respectively, clearly point out that compound **2** is an excellent AIEgen for potential optoelectronic applications. Although **2** and **4** are electronically equal, the presence of the octyl chains in **2** clearly plays a crucial role in the intermolecular organization of the system that impacts its PL in the solid state. On the contrary, **4** showed weak emission in the solid state.

As we mentioned previously, one of the main challenges is the development of luminescent boron cluster-based fluorophores for biomedicine.[10] Nevertheless, this is not attainable for those compounds that have low solubility in water or undergo quenching of the light emission in solution.

Table 1 Photophysical properties of **1–6** in different states (solution, aggregate, solid, NPs and films)

Compounds	λ_{abs}[a] (nm)	$\varepsilon/10^5$ (M^{-1} cm^{-1})	λ_{em}[a] (nm)	Φ_{PL}[a]	λ_{em}[b] (nm)	Φ_{PL}[b]	λ_{em}[c] (nm)	Φ_{PL}[cd]	λ_{em}[e] (nm)	Φ_{PL}[e]	λ_{em}[f] (nm)	Φ_{PL}[fd]
1	349	2.690	372, 393	0.89	380	<0.01	435	0.08	—	—		
2	286, 314	0.542, 0.611	404	0.01	483	0.06	477	0.71	478	0.39	473	0.74
3	346	2.322	367, 389	0.64	465	0.04	511	0.18	—	—		
4	293, 308	0.522, 0.572	372	< 0.01	536	0.01	500	0.04	528	0.01	546	0.03
5	348	0.2614	389, 407	0.25	452	0.03	—	—	—	—		
6	274	0.3211	390	0.19	—	—	591	0.10	—	—		

[a] THF solutions (3.0×10^{-5} M for **2**, **4–6** and 1×10^{-6} M for **1** and **3**). [b] In the aggregate state (THF/H_2O = 1/99 (v/v)). [c] In the solid state. [d] Absolute Φ_{PL} from the integrating sphere. [e] NPs of **2** and **4** in water suspensions. [f] Thin films prepared by spin-coating of THF solutions on Spectrosil B quartz substrates.

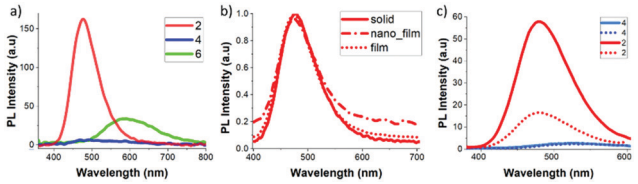

Fig. 2 (a) PL spectra of **2**, **4** and **6** in the solid state. (b) Normalised PL spectra of **2** as a solid, film and NPs in a film. (c) Fluorescence emission spectra of aggregates in THF/H_2O (1 : 99, v/v) (dotted lines) and NPs in water (solid lines) at 1×10^{-5} M of **2** and **4** (λ_{exc} = 314 nm).

To overcome this problem, we have successfully prepared water-dispersible and water-stable carborane-containing organic NPs from our fluorophores. For this purpose, we have optimized the reprecipitation method dropping a concentrated solution of a water miscible organic solvent (THF) of the flourophore in a large amount of water under vigorous stirring to obtain stable NPs (see the ESI‡ for details).[13] To obtain a NP suspension in pure water for biological applications the THF is remove by dialysis (stirred at r.t. for 72 h). According to transmission electron microscopy (TEM), NPs were obtained for **2**, **4** and **6**, with sizes in the range from 70 nm to 100 nm (Fig. 3a and b, and Fig. S21, ESI‡). Dynamic light scattering (DLS) (Fig. S22 and Table S14, ESI‡) showed an average size distribution in the range from 72 nm to 122 nm, which matches quite well with TEM, with low PDI values (0.09–0.12). For **2**, the *Z* potential value of –43.6 mV, clearly indicates the high stability of the colloidal suspension, confirmed by TEM and DSL measurements of NPs stored at 4 °C for two weeks. In particular, compound **2**, having the more impeded aromatic systems, provided the NPs with the highest emission (Fig. 3c). These NPs showed a maximum at 478 nm that perfectly matches with that of the aggregates (Fig. 2c). A significant fluorescence enhancement with a Φ_{PL} = 0.39 was observed compared to the solution state. Also, the luminescence properties of NPs of **2** have been confirmed by fluorescence microscopy (Fig. 3d). This is an important breakthrough for this type of carborane cluster-based material, which is not luminescent in solution but shows outstanding AIE phenomena in the solid state enabling its use in other motivating applications such as bio(nano)medicine.

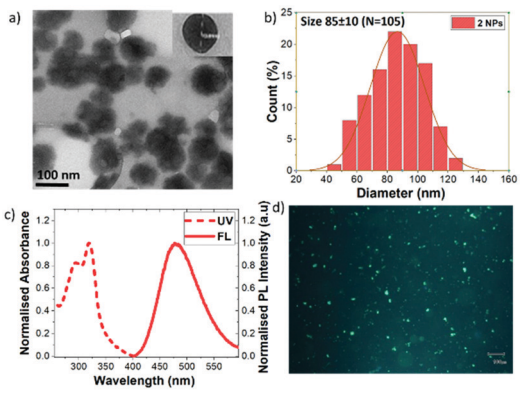

Fig. 3 (a) TEM image of NPs. (b) Size distribution histogram for NPs of **2**. (c) Normalised absorption and emission spectra of suspensions of NPs of **2** in H_2O (λ_{exc} = 314 nm). (d) Fluorescence microscopy image from NPs of **2** in 10% FBS (fetal bovine serum) and 1% DMSO (λ_{exc} = 330–385 nm).

Furthermore, films doped with NPs could be appealing for solar cells incorporating luminescent solar concentrators (LSCs) because they exhibit strong UV absorption and a down-shifted PL that can be better matched to the absorption spectrum of the photovoltaic cell.[14] As a proof of concept, thin films were prepared by drop-casting an aqueous dispersion of NPs of **2** (10^{-3} M) on Spectrosil B quartz substrates and allowing them to dry under ambient conditions. Noticeably, an outstanding Φ_{PL} of 0.54 was obtained from films of NPs, which is comparable or even higher to quantum yields of previously reported LSC dyes.[15]

In conclusion, this study demonstrates that water insoluble *o*-carborane-based fluorophores can be dispersed in water by preparing NPs unprecedentedly, in a controlled manner. We have proved that the fluorenyl derivative **2**, with octyl groups, is an excellent AIEgen in the solid state (Φ_{PL} = 0.71) and processed as thin films (Φ_{PL} = 0.74). More importantly, the luminescence properties are preserved when the material is in the form of water-dispersible NPs (Φ_{PL} = 0.39). Additionally, NPs deposited on Spectrosil B quartz substrates also showed an outstanding fluorescence efficiency (Φ_{PL} = 0.54). Thus, we have demonstrated that *o*-carborane-based fluorenes can be luminescent materials both in the solid state and in aqueous media as dispersible NPs. Further, NPs processed as thin films can be potentially useful in electronic devices as sensors and solar cells. These results open up new opportunities for the use of these types of systems both in biomedicine and electronic devices. Research work is currently underway in these directions.

This work was financially supported by MICINN (PID2019-106832RB-I00, PID2019-105622RB-I00 and the Severo Ochoa Program for Centers of Excellence for the FUNFUTURE CEX2019-000917-S project). S. S. acknowledges financial support from DOC-FAM, the European Union's Horizon 2020 research and innovation programme under the Marie Sklodowska-Curie grant agreement No 754397. Z. K. is grateful for the general support of the Premium Postdoctoral Research Program 2019. We thank Dr Claudio Roscini from ICN2 for his kind help with the solid state luminescence measurements. Sohini Sinha is enrolled in the UAB PhD Program.

Conflicts of interest

There are no conflicts to declare.

References

1 (*a*) C. Adachi, R. Hattori and H. Kaji, in *Handbook of Organic Light-Emitting Diodes*, ed. T. Tsujimura, Springer, Tokyo, Japan, 2020; (*b*) M. Koden, *OLED Displays and Lighting*, John Wiley & Sons, Ltd., Hoboken, NJ, 2017; (*c*) Y. Jiang, Y.-Y. Liu, X. Liu, H. Lin, K. Gao, W.-Y. Lai and W. Huang, *Chem. Soc. Rev.*, 2020, **49**, 5885.

2 (*a*) M. Yamaguchi, S. Ito, A. Hirose, K. Tanaka and Y. Chujo, *Mater. Chem. Front.*, 2017, **1**, 1573; (*b*) H. Zhang, Z. Zhao, A. T. Turley, L. Wang, P. R. McGonigal, Y. Tu, Y. Li, Z. Wang, R. T. K. Kwok, J. W. Y. Lam and B. Z. Tang, *Adv. Mater.*, 2020, **32**, 2001457; (*c*) S. P. Fisher, A. W. Tomich, S. O. Lovera, J. F. Kleinsasser, J. Guo, M. J. Asay, H. M. Nelson and V. Lavallo, *Chem. Rev.*, 2019, **119**, 8262–8290.

3 (*a*) K.-R. Wee, Y.-J. Cho, S. Jeong, S. Kwon, J.-D. Lee, I.-H. Suh and S. O. Kang, *J. Am. Chem. Soc.*, 2012, **134**, 17982–17990; (*b*) A. R. Davis, J. J. Peterson and K. R. Carter, *ACS Macro Lett.*, 2012, **1**, 469–472; (*c*) J. Guo, D. Liu, J. Zhang, J. Zhang, Q. Miao and Z. Xie, *Chem. Commun.*, 2015, **51**, 12004–12007; (*d*) R. Furue, T. Nishimoto, I. S. Park, J. Lee and T. Yasuda, *Angew. Chem., Int. Ed.*, 2016, **55**, 7171–7175; (*e*) J. Ochi, K. Tanaka and Y. Chujo, *Angew. Chem., Int. Ed.*, 2020, **59**, 9841–9855.

4 (*a*) S. Y. Kim, J. D. Lee, Y. J. Cho, M. R. Son, H. J. Son, D. W. Cho and S. O. Kang, *Phys. Chem. Chem. Phys.*, 2018, **20**, 17458–17463; (*b*) X. Wu, J. Guo, Y. Quan, W. Jia, D. Jia, Y. Chen and Z. Xie, *J. Mater. Chem. C*, 2018, **6**, 414–4149; (*c*) X. Wu, J. Guo, Y. Cao, J. Zhao, W. Jia, Y. Chen and D. Jia, *Chem. Sci.*, 2018, **9**, 5270–5277; (*d*) D. S. Tu, S. Z. Cai, C. Fernandez, H. L. Ma, X. Wang, H. Wang, C. Q. Ma, H. Yan, C. S. Lu and Z. F. An, *Angew. Chem., Int. Ed.*, 2019, **58**, 9129; (*e*) K. L. Martin, J. N. Smith, E. R. Young and K. R. Carter, *Macromolecules*, 2019, **52**, 7951–7960.

5 (*a*) J. Poater, C. Viñas, I. Bennour, S. Escayola, M. Solà and F. Teixidor., *J. Am. Chem. Soc.*, 2020, **142**, 9396–9407; (*b*) R. Núñez, *et al.*, *Chem. – Eur. J.*, 2013, **19**, 17021–17030; (*c*) L. Weber, J. Kahlert, R. Brockhinke, L. Bçhling, A. Brockhinke, H.-G. Stammler, B. Neumann, R. A. Harder and M. A. Fox, *Chem. – Eur. J.*, 2012, **18**, 8347–8357; (*d*) J. Kahlert, H.-G. Stammler, B. Neumann, R. A. Harder, L. Weber and M. A. Fox, *Angew. Chem., Int. Ed.*, 2014, **53**, 3702–3705.

6 (*a*) R. Núñez, P. Farràs, F. Teixidor, C. Viñas, R. Sillanpää and R. Kivekäs, *Angew. Chem., Int. Ed.*, 2006, **45**, 1270–1272; (*b*) F. Teixidor, R. Núñez, C. Viñas, R. Sillanpää and R. Kivekäs, *Angew. Chem., Int. Ed.*, 2000, **39**, 4290–4292; (*c*) J. O. Huh, H. Kim, K. M. Lee, Y. S. Lee, Y. Do and M. H. Lee, *Chem. Commun.*, 2010, **46**, 1138–1140; (*d*) A. M. Spokoyny, C. W. Machan, D. J. Clingerman, M. S. Rosen, M. J. Wiester, R. D. Kennedy, C. L. Stern, A. A. Sarjeant and C. A. Mirkin, *Nat. Chem.*, 2011, **3**(8), 590.

7 (*a*) B. P. Dash, R. Satapathy, E. R. Gaillard, K. M. Norton, J. A. Maguire, N. Chug and N. S. Hosmane, *Inorg. Chem.*, 2011, **50**, 5485–5493; (*b*) S. Kwon, K.-R. Wee, Y.-J. Cho and S. O. Kang, *Chem. – Eur. J.*, 2014, **20**, 5953–5960; (*c*) R. Núñez, *et al.*, *Chem. – Eur. J.*, 2014, **20**, 9940–9951; (*d*) L. Zhu, W. Lv, S. Liu, H. Yan, Q. Zhao and W. Huang, *Chem. Commun.*, 2013, **49**, 10638; (*e*) D. Tu, P. Leong, S. Guo, H. Yan, C. Lu and Q. Zhao, *Angew. Chem., Int. Ed.*, 2017, **56**, 11370–11374; (*f*) H. Naito, K. Nishino, Y. Morisaki, K. Tanaka and Y. Chujo, *Angew. Chem., Int. Ed.*, 2017, **56**, 254–259; (*g*) H. Mori, K. Nishino, K. Wada, Y. Morisaki, K. Tanaka and Y. Chujo, *Mater. Chem. Front.*, 2018, **2**, 573–579.

8 (*a*) H. So, J. H. Kim, J. H. Lee, H. Hwang, D. K. An and K. M. Lee, *Chem. Commun.*, 2019, **55**, 14518–14521; (*b*) M. Kim, C. H. Ryu, J. H. Hong, J. H. Lee, H. Hwang and K. M. Lee, *Inorg. Chem. Front.*, 2020, **7**, 4180–4189.

9 (*a*) J. M. Oliva, N. L. Allan, P. V. R. Schleyer, C. Viñas and F. Teixidor, *J. Am. Chem. Soc.*, 2005, **127**, 13538–13547; (*b*) R. Núñez, *et al.*, *Chem. – Eur. J.*, 2012, **18**, 544–553; (*c*) K.-R. Wee, Y.-J. Cho, J. K. Song and S. O. Kang, *Angew. Chem., Int. Ed.*, 2013, **52**, 9682–9685; (*d*) J. Ochi, K. Tanaka and Y. Chujo, *Dalton Trans.*, 2021, **50**, 1025.

10 (*a*) R. Núñez and C. Prandi, *et al.*, *Chem. – Eur. J.*, 2018, **24**, 15622–15630; (*b*) M. Chaari, Z. Kelemen, D. Choquecillo-Lazarte, N. Gaztelumendi, C. Nogués, F. Teixidor, C. Viñas and R. Núñez, *Biomater. Sci.*, 2019, **7**, 5324–5337.

11 (*a*) S.-Y. Kim, A.-R. Lee, G. F. Jin, Y.-J. Cho, H.-J. Son, W.-S. Han and S. O. Kang, *J. Org. Chem.*, 2015, **80**, 4573–4580; (*b*) Z. Wang, T. Wang, C. Zhang and M. G. Humphrey, *Phys. Chem. Chem. Phys.*, 2017, **19**, 12928–12935; (*c*) N. Shin, S. Yu, J. H. Lee, H. Hwang and K. M. Lee, *Organometallics*, 2017, **36**(8), 1522–1529; (*d*) Z. Wang, T. Wang, C. Zhang and M. G. Humphrey, *ChemPhotoChem*, 2018, **2**, 369–379; (*e*) X. Wu, J. Guo, Y. Lv, D. Jia, J. Zhao, H. Shan, X. Jin and Y. Ma, *Mater. Chem. Front.*, 2020, **4**, 257–267; (*f*) D. K. You, H. So, C. H. Ryu, M. Kim and K. M. Lee, *Chem. Sci.*, 2021, **12**, 8411–8423.

12 (*a*) K. Sonogashira, Y. Tohda and N. Hagihara, *Tetrahedron Lett.*, 1975, 4467–4470; (*b*) R. Conway-Kenny, A. Ferrer-Ugalde, O. Careta-Borràs, X. Cui, J. Zhao, C. Nogués, R. Núñez, J. Cabrera-González and S. M. Draper, *Biomater. Sci.*, 2021, **9**, 5691–5702.

13 D. Blasi, D. M. Nikolaidou, F. Terenziani, I. Ratera and J. Veciana, *Phys. Chem. Chem. Phys.*, 2017, **19**, 9313.

14 Michael G. Debije and Paul P. C. Verbunt, *Adv. Energy Mater.*, 2012, **2**, 12–35.

15 H.-Y. Huang, K.-B. Cai, Y.-R. Sie, Kai Li, J.-M. Yeh and C.-T. Yuan, *Sol. RRL*, 2019, **3**, 1800347.